28

ИНСТИТУТ ЯДЕРНОЙ ФИЗИКИ СО АН СССР

O.K. Vorov, V.G. Zelevinsky

QUARTIC ANHARMONICITY AND ANGULAR MOMENTUM EFFECTS IN EVEN-EVEN SPHERICAL NUCLEI

PREPRINT 84-137

НОВОСИБИРСК

O.K. Vorov, V.G. Zelevinsky

QUARTIC ANHARMONICITY AND ANGULAR MOMENTUM EFFECTS IN EVEN-EVEN SPHERICAL NUCLEI

A B S T R A C T

Arguments are given that the main nonlinear features of low-lying quadrupole excitations of even-even soft spherical nuclei are due to the quartic phonon interaction and to the coherent rotational response of noncollective degrees of freedom. The corresponding Hamiltonian is solved by group theory methods; results give a good description of energy spectra as well as of transition probabilities, number of fitted parameters being less than that of IBA. Some regularities are found going through the periodical table.

1. Introduction

The great success of interacting boson approximation (IBA) firstly introduced in [1, 2] and reformulated and studied in detail in [3—5] has animated the interest to the description of low-lying nuclear states in terms of elementary boson excitations. However the impartial observer has to note that the original simplicity and attractiveness of IBA disappeared gradually with the number of fitted parameters increasing. Specific features of IBA (identification of bosons with fermion pairs, boson number conservation, taking into account s- and d-bosons only) are proved to be weakest points of the whole approach and have obtained neither experimental nor theoretical justification [6].

Below we limit ourselves mainly by soft spherical even-even nuclei. The microscopical boson expansion technique (BET) was shown [7] to be able to describe experimental data for typical nuclei of that kind (Ru and Pd isotopes) quite satisfactorily. But the BET is connected with complicated numerical calculations and the procedure is not unique. Of course it is always possible to diagonalize the pure phenomenological boson Hamiltonian [8, 9]. For Ru isotopes such a calculation [10] fits data better than IBA. This manifests that the usual quadrupole boson scheme with anharmonicity in principle does reproduce all the picture. The goal of this work is to find out which anharmonic terms are most important ones and to demonstrate some regularities generated by their dominance.

2. The dominance of quartic anharmonicity

Bohr—Mottelson phenomenology of quadrupole motion based on two ideas: (i) the collective nature of states under consideration (their wave functions $\Psi = \sum_i c_i \varphi_i$ are coherent sums of $\Omega \gg 1$ contributions of simple excitations φ_i, $c_i \sim \Omega^{-1/2} \ll 1$ so that each simple mode is weakly distorted by collective motion) and (ii) the collective motion is rather slow that its frequency $\omega \ll 2\bar{E}$, the energy of pair breaking. Actually in soft nuclei one has

$$\tau \equiv \frac{\omega}{2E} \lesssim \Omega^{-1/3} . \tag{1}$$

Using parameters Ω and τ one can estimate roughly the anharmonic effects. The quasiparticle-phonon coupling constant γ can be deduced

from equating the phonon propagator $1/\omega$ to the RPA two-quasiparticle loop $\sim\gamma\Omega/E^3$. It gives $\gamma^2\sim\omega^2/\Omega\tau^3$, or, from (1), $\gamma\sim\omega$. Therefore, the quasiparticle-phonon interaction is strong for soft-mode phonons. This coupling induces n-phonon loops $H^{(n)}$ which can be estimated as

$$H^{(n)}\sim\gamma^n\Omega E\frac{1}{E^n}\sim\omega\Omega\tau^{n-1}. \tag{2}$$

According to (1), cubic $H^{(3)}$ and quartic $H^{(4)}$ anharmonic terms are strong whereas higher terms $H^{(n>4)}$ are relatively weak compared with ω and can be treated as perturbations.

Moreover, it can be shown that $H^{(3)}$ (as well as higher odd-order terms) contains as additional depression factor due to the approximate particle-hole symmetry near the Fermi surface. In macroscopic systems such contributions vanish analogously to the Furry theorem in QED. Thus, one can expect that the pattern of spectra is determined mainly by the quartic anharmonicity $H^{(4)}$. At $\tau\ll1$ one should keep only the coordinate part ($\sim\beta^4$) of $H^{(4)}$. Since four quadrupole bosons have only one spin 0-state the structure of $H^{(4)}$ is unique and contains only one constant [11, 12].

So one can start with the simple Hamiltonian

$$H_0=H_{harm}+H^{(4)}=\omega\sum_\mu\left(d_\mu^+d_\mu+\frac{1}{2}\right)+\frac{\omega\lambda}{4}\left[\sum(-1)^\mu d_\mu^{(+)}d_{-\mu}^{(+)}\right]^2 \tag{3}$$

where Bose-operators d_μ and d_μ^+ are introduced and collective coordinates α_μ and momenta π_μ are defined as

$$\alpha_\mu=\frac{1}{\sqrt{2\omega}}[d_\mu+(-1)^\mu d_{-\mu}^+]\equiv\frac{1}{\sqrt{2\omega}}d_\mu^{(+)}, \tag{4a}$$

$$\pi_\mu=-i\sqrt{\frac{\omega}{2}}[d_\mu-(-1)^\mu d_{-\mu}^+]\equiv-i\sqrt{\frac{\omega}{2}}d_\mu^{(-)} \tag{4b}$$

3. The solution of the problem

The Hamiltonian (3) does not conserve the boson number N_B. Nevertheless it gives the SU(5)-pattern of spectra. It can be shown [12], without numerical calculations, by means of the variational method which gives even in the simplest approximation results of high precision. The method was used for the first time apparently in Ref. [11] and afterwards was rediscovered by many authors (for example, [13, 14] for various nonlinear quantum problems. The method consists of the

boson operator canonical transformation which corresponds to the optimum choice of the boson mean field (the condensate of boson pairs with the angular momentum $J=0$). The remarkable property of the Hamiltonian (3) is its five-dimensional rotational invariance (O(5)-symmetry). The corresponding constant of motion is the seniority v (number of nonpaired bosons).

Introducing the generators of the SO(2,1) group

$$P=\frac{1}{2}\sum_\mu(-1)^\mu d_\mu d_{-\mu}, \quad P^+=\frac{1}{2}\sum(-1)^\mu d_\mu^+ d_{-\mu}^+ \tag{5a}$$

and

$$P_0=\frac{1}{2}\left(N+\frac{5}{2}\right)=\frac{1}{2}\left(v+2n+\frac{5}{2}\right) \tag{5b}$$

where n is condensate boson pair number one reduces the Hamiltonian (3) to the simple form

$$H_0=\omega[2P_0+\lambda(2P_0+P+P^+)^2] \tag{6}$$

Then one carried out the canonical transformation

$$P=\frac{1}{4}\left(\sqrt{\omega_v}+\frac{1}{\sqrt{\omega_v}}\right)^2\tilde{P}+\frac{1}{4}\left(\sqrt{\omega_v}-\frac{1}{\sqrt{\omega_v}}\right)^2\tilde{P}^+-\frac{1}{2}\left(\omega_v-\frac{1}{\omega_v}\right)\tilde{P}_0, \tag{7a}$$

$$P_0=\frac{1}{2}\left(\omega_v+\frac{1}{\omega_v}\right)\tilde{P}_0-\frac{1}{4}\left(\omega_v-\frac{1}{\omega_v}\right)\left(\tilde{P}+\tilde{P}^+\right) \tag{7b}$$

in each subspace with v fixed separately. The dimensionless variational parameter $\omega_v\to1$ should be determined from the condition of compensation for «dangerous» graphs in the transformed Hamiltonian $H(\tilde{P},\tilde{P}^+,\tilde{P}_0)$,

$$\omega_v^3-\omega_v=4\left(v+\frac{7}{2}\right)\lambda. \tag{8}$$

The low-lying states are labelled now by quantum numbers $|v,\tilde{n},J,M\rangle$ and the energy spectrum can be expressed as

$$\frac{E_{vn}}{\omega}=\frac{1}{4}\left(3\omega_v+\frac{1}{\omega_v}\right)\left(v+\frac{5}{2}\right)+$$

$$+2\omega_v\tilde{n}\left\{1+\tilde{\lambda}_v\left[3(\tilde{n}-1)+v+\frac{7}{2}\right]\right\}+O(\tilde{\lambda}_4^2) \tag{9}$$

where the renormalized coupling constant $\tilde{\lambda}_v$ is small

$$\tilde{\lambda}_v = \frac{\lambda}{\omega_v^3} = \frac{1-\omega_v^{-2}}{4(v+7/2)} \leqslant \frac{1}{4(v+7/2)} \leqslant \frac{1}{14} \qquad (10)$$

Residual terms in eq.(9) give small admixtures of states with the same v and $\tilde{n}' = \tilde{n} \pm 1$, $\tilde{n} \pm 2$. For the case of actual interest ($n=0$ or $n=1$) eq.(9) without residual terms guarantees the level energy within the accuracy better than 1%. Hence, we keep the SU(5)-classification of low levels (for each v) at arbitrary strong quartic anharmonicity.

4. Yrast-spectra and angular momentum effects

The yrast-spectrum $E_J(\tilde{n}=0,\ 2v=J)$ is given by the first term of eq.(9). It changes from the equidistant one, $E_J = E_0 + \frac{\omega}{2}J$, in the harmonic limit ($\lambda=0$) to

$$E_J = \frac{3}{8}\omega(J+5)[2(J+7)\lambda]^{1/3} \qquad (11)$$

for the strong anharmonicity when $4\left(v+\frac{7}{2}\right)\lambda \gg 1$, $\omega_v \approx \left[4\left(v+\frac{7}{2}\right)\lambda\right]^{1/3}$. At not very high J (11) coincides practically with the phenomenological expression $E_J = E_0 + \alpha J + \beta J^2$ suggested in [15] and with the corresponding limit of IBA. For higher J one obtains from (11) $E_J \sim J^{4/3}$ as in the variable moment of inertia (VMI) model [16, 17]. In table 1 we compare the asymptotical predictions (11) with yrast-spectra [18] of typical spherical nuclei ^{100,102}Pd. Let us note that for the energy ratios $R_J = (E_J - E_0)/(E_2 - E_0)$ eq.(11) is parameter-free.

We see that the asymptotical formula (8) exactly describes the yrast-band of ^{100}Pd without any parameters. As for the spectrum of ^{102}Pd, deviations of R_J from the asymptotical value R_J^{00}, eq.(11), can be described by one constant $\sigma = 0.012 \pm 0{,}001$ corresponding in the absolute scale to energy shifts $(6.6 \pm 0.7)J(J+1)$ keV. Isotopes ^{98}Ru and ^{102}Cd show yrast-bands similar to that of ^{100}Pd (all these nuclei have $N=54$, i.e. four valence neutrons). Deviations from R_J^{00} are small for ^{132}Xe ($N=78$, four neutron holes), ^{140}Xe ($N=86$, four neutrons in the next major shell) as well as transitional nuclei with $N=86$ (^{148}Sm and ^{150}Gd) and $N=88$ (^{152}Gd and ^{154}Dy).

5. General trends of yrast-spectra

One can try to describe general trends of low-lying yrast-spectra with one-parameter interpolation

$$R_J = R_J^{00} + \sigma J(J+1), \quad J \geqslant 4 . \qquad (12)$$

This simple parametrization gives reasonable description (up to the back-bending region) for soft spherical as well as for well deformed nuclei and σ is changing regularly from one nucleus to another. In Fig.1 the values of $w = \sigma(E_2 - E_0)$ are shown for vibrational nuclei Pd, Ru, Cd. For near-magic isotopes ($N=52$) one obtains $w \sim -10$ keV. With N increasing w crosses zero (for those isotopes $R_J \approx R_J^{00}$) and rather soon becomes approximately constant, $w \approx$ (8—9) keV. The behaviour is similar for isotopes of Xe and Ba. Errors of fits are connected with the dispersion of σ values extracted with the aid of different number of yrast levels. These errors increase significantly in near-magic nuclei where $w < 0$.

The similar picture is proved to take place in the next neutron major shell (isotopes of Sm, Gd, Dy and Er), Fig.2. Again one obtains in near-magic nuclei ($N=84$) $w \approx -$ (10—13) keV, then w grows steeply followed by platean-like region where $w \approx 6$—7 keV. The same is approximately valid for isotopes of Ce and Ne. For isotopes crossing a neutron closed shell at neutron number increasing, one seen roughly a symmetry with respect to the magic number with deeply negative values of w for $N = N_{magic}$. In spite of the stable deformation typical to nuclei with $N \to 90$ their yrast-band behaviour, from the viewpoint of the parametrization (12), is quite analogous to that of soft spherical nuclei.

Heavy nuclei (isotopes of Th, U and transuranic elements) show approximately constant values of $w \approx 3$—4 keV. Thus, practically all yrast-bands of nonmagic medium and heavy nuclei can be described by eq.(12) the quantity $wJ(J+1)$ being close to the rigid-body rotational energy, $\hbar^2/2w \approx T_{rig}$, rigid-body moment of inertia. It is well known that the kinetic energy of H_{harm}, eq.(3), contains the rotational contribution with small hydrodynamic moments of inertia $\sim\beta^2$ We see that two important parts should be added to the harmonic Hamiltonian to achieve the qualitative agreement with data: (i) quartic anharmonicity and (ii) rigid rotation. Since the description covers also yrast-bands of well deformed nuclei where total moments of inertia are equal, due to pairing correlations, to $T \approx (1/2$—$1/3)T_{rig}$ one can interpret the interpolation (12) as subdivision of rotational contributions into rigid-body and hydrodynamical ones. Therefore one can speculate that the main

effects of superfluid pair correlations are accumulated in the quartic anharmonicity (for nuclei with a soft quadrupole mode, eq, (1)).

The microscopic theory of large amplitude quadrupole vibration predicts [19, 20] such rotational contributions as consequence of the coherent response of noncollective degrees of freedom to slow quadrupole deformation. Calculations using BET neglect usually such terms and consider mainly high order contributions to potential energy (3).

There are some deviations from the systematics considered. It fails for isotopes of Te (for ^{120,122}Te $w \approx 0$ and $w < 0$ for other isotopes). The average value of w for isotopes Os, Pt and Hg is higher than obtainable from T_{rig}. Probably it is a consequence of the effective nonaxiality typical for this group of nuclei [21, 22]. Here it is necessary to take into account the sextic anharmonicity $\sim\beta^6 \cos^2 3\gamma$. Terms $\sim\beta^6$ are important also in cases of abnormal smallness of quartic constant λ and in unstable situation with $\lambda < 0$. The sign of λ is not fixed by the microscopic theory; it is determined by the counterplay of p—p (h—h) and p—h interactions. The region $\lambda < 0$ where $H^{(6)}$ is crucial for restoring the stability can be the connected with the long-standing problem of low-lying 0^+ states in some isotopes of Ge, Se and Mo. Letting alone these 0^+ levels one can see that in general isotopes of Se, Kr and Sr also obey the common rules.

6. An illustrative example: Pd isotopes

Having established the general picture one can try to reproduce not only yrast states (here eq. (12) is rather close to VMI description) but the whole pattern of low-lying spectra including side bands. The family of isotopes ^{98}Pd—^{110}Pd was chosen as an appropriate sample due to abundance of data. We have used for comparison (Table 2) yrast levels up to $J = 14$, γ-bands and side band levels with boson number $N_B \leqslant 3$ i.e. almost all known low-lying levels. All these levels apparently are of collective nature justifying the applicability of the model. Experimental data were taken mostly from [23]; data taken from other papers [24, 25, 26] are indicated in Table 2.

We followed the very simple procedure fitting σ in (12) for yrast levels and then using this value to calculate R_J for other states by eq. (12) where R_J^{00} should be replaced by the corresponding expression following from eqs (8—12) in asymptotical limit. This one-parameter fit was compared with the IBA-type fit carried out with three-parameter formula

$$R_J = N_B + \langle N_B, v, J \Big| \sum_{L=0,2,4} \frac{1}{2} \sqrt{2L+1}\, C_L((d^+ d^+)_L (dd)_L)_{00} \Big| N_B, v, J \rangle \qquad (13)$$

with boson number N_B conserved [5]. We show in Table 2 results as triplets of R_J for each level where the upper line gives our calculations (quartic anharmonicity angular momentum model of anharmonic vibration, QAAM), the middle line shows an experimental data and the lower line corresponds to IBA calculation (13). In the IBA-case parameters C_0, C_2 and C_4 were fitted by the least square method for each isotope independently.

Fig.3 shows the mean square deviations $\frac{1}{N}\sum_{i=1}^{N}(R_i^{th} - R_i^{exp})^2$ as function of neutron number for QAAM and IBA calculations. For all isotopes except ^{106}Pd and ^{108}Pd the one-parameter QAAM-description gives better agreement than the three-parameter IBA-fit. One should note that there is only few levels known in ^{108}Pd. At Fig.4 we show values of fitted parameters for two versions. Obviously, the QAAM-parameter σ is a quite regular function of the shell occupation. As we have mentioned above, the similar behavior of σ exists almost in all nuclei except magic ones.

7. Allowed quadrupole transitions

To calculate the transition probabilities one need to know the wave functions of stationary states. In the same approximation as for energies (9) one can express these functions $|v\,\tilde{n}, J, M\rangle$ as expansions over standart independent phonon states $|v, n, J, M\rangle_0$,

$$|v, \tilde{n}, J, M\rangle = \sum_m A^v_{nm} |v, m, J, M\rangle \qquad (14)$$

where overlap coefficients are

$$A^v_{nm} = \sqrt{\frac{\Gamma(n+v+5/2)\,\Gamma(m+v+5/2)}{n!\,m!\,[\Gamma(v+5/2)]^2}}\,(-1)^m a_v^{v+5/2} b_v^{n+m} \times$$

$$\times F\left(-m, -n; v+\frac{5}{2}; \frac{b_v^2-1}{b_v^2}\right) \qquad (15)$$

where F is a gypergeometric function and

$$a_v = \frac{2\sqrt{\omega_v}}{\omega_v+1}, \qquad b_v = \frac{\omega_v - 1}{\omega_v + 1}. \qquad (16)$$

Then one have to take the harmonic approximation matrix elements and to sum very rapidly convergent series with coefficients (15).

It is easy to show that the main contributions to the E2-transition operator Q have the same operator structure as $\delta H/\delta Q_{\mu}$. In our Hamiltonian H_0 (3) we have neglected odd-order anharmonic effects. Therefore it will self-consistent to consider enhanced (allowed in the harmonic approximation) E2-transitions only. Taking into account angular momentum effects (12) we have to postulate a phenomenological two-parameter E2-operator

$$Q_{\mu}=d^{(+)}_{\mu}+\varkappa((d^{(+)2})_0 d^{(+)})_{2\mu}+\frac{k}{2}([d^{(-)}, J]_+)_{2\mu}\,. \tag{17}$$

Then the transition probabilities ($\Delta N_B=1$) between the lowest states are

$$B(E2; 2^+_1\to 0^+_1)=K_0\left|1+\frac{14\varkappa}{\sqrt{5}\,(\omega_0+\omega_1)}+\sqrt{\frac{3}{2}}k\omega_0\right|^2, \tag{18}$$

$$B(E2; 4^+_1\to 2^+_1)=2K_1\left|1+\frac{18\varkappa}{\sqrt{5}\,(\omega_1+\omega_2)}+\frac{7}{\sqrt{6}}k\omega_1\right|^2, \tag{19}$$

$$B(E2; 2^+_2\to 2^+_1)=2K_1\left|1+\frac{18\varkappa}{\sqrt{5}\,(\omega_1+\omega_2)}\right|^2, \tag{20}$$

$$B(E2; 0^+_2\to 2^+_1)=\frac{2}{\omega_1}(K_0\omega_0)^{9/7}\times$$

$$\times\left|1-\frac{5}{4}\varepsilon+\frac{28}{\sqrt{5}}\frac{1-5\varepsilon/8}{\omega_0+\omega_1}\varkappa-\sqrt{\frac{3}{2}}\left(1+\frac{9}{4}\varepsilon\right)k\omega_0\right|^2 \tag{21}$$

where

$$K_v=\frac{1}{\omega_v}\left(\frac{2\sqrt{\omega_v\omega_{v+1}}}{\omega_v+\omega_{v+1}}\right)^{2v+7}, \qquad \varepsilon=\frac{\omega_1-\omega_0}{\omega_0}\,. \tag{22}$$

Table 3 shows the experimental data ([27, 7] and references therein) for relative probabilities (19—20) in isotopes $^{102-110}$Pd

$$\beta_J=\frac{B(E2; J^+\to 2^+_1)}{B(E2; 2^+_1\to 0^+_1)} \tag{23}$$

in units of one-phonon probabilities (18). Those are compared with corresponding model predictions. Data are reproduced reasonably well with parameters $\varkappa$ and k changing smoothly from one isotope to another. Parameter k is actually constant and values $\varkappa$ and k are in rough agreement with the estimate from $\delta H/\delta Q_{2\mu}$. Let us outline that we carried out all calculations in the strong coupling limit (asymptotical approximation with respect to the quartic anharmonicity constant λ; as a result λ drops out from formulae. Refusing this approximation one acquires an additional parameter. But it is hardly worthwhile to make such a complication without taking into account cubic anharmonic effects simultaneously. Latter are necessary to describe forbidden E2-transitions, mean values of the quadrupole momentum [12] and M1-transitions.

Here we did not try to present an exact calculation for the complete set of data. We would like rather to demonstrate that moving along the classical phenomenological path and using the microscopic grounds to extract the main anharmonic effects one can understand general trends and stress qualitative regularities distinctly. Certaintly the total description of collective quadrupole motion in soft spherical nuclei could be achieved by the consistent microscopic theory only.

REFERENCES

1. *D. Janssen, F. Donau, S. Frauendorf and R.V. Jolos.* Nucl. Phys. A172 (1971) 145.
2. *D. Janssen, R.V. Jolos and F. Donau.* Nucl. Phys. A224 (1974) 93.
3. *F. Iachello and A. Arima* Phys. Lett. 53B (1974) 309.
4. *A. Arima and F. Iachello.* Phys. Rev. Lett. 35 (1975) 1069.
5. *A. Arima and F. Iachello.* Ann. Phys. (N.Y.) 99 (1976) 253.
6. *V.G. Zelevinsky.* Preprint INP, 83-56. Novosibirsk (1983).
7. *K. Weeks and T. Tamura.* Phys. Rev. C22 (1980) 888.
8. *G. Gneuss, U. Mosel and W. Greiner.* Phys. Lett. 30B (1969) 397; 31B (1970) 209; 32B (1970) 161.
9. *G. Gneuss and W. Greiner.* Nucl. Phys. A171 (1971) 449.
10. *S.G. Lie and G. Holzwarth.* Phys. Rev. C12 (1975) 1035.
11. *V.G. Zelevinsky.* JETP 46 (1964) 1853.
12. *O.K. Vorov and V.G. Zelevinsky.* Yad. Fiz. 37 (1983) 1392.
13. *L.D. Mlodinov and N. Papanicolaov.* Ann. of Phys. (N.Y.) 128 (1980) 314.
14. *E.D. Feranchuk and L.J. Komarov.* Phys. Lett. 88A (1982) 211.
15. *H. Ejiri et al.* J. Phys. Soc. Japan 24 (1968) 1189.
16. *M.A.J. Mariscotti, G. Scharff-Goldhaber and B. Buck.* Phys. Rev. 178 (1969) 1864.
17. *G.Scharff-Goldhaber and A.S. Goldhaber.* Phys. Rev. Lett. 24 (1970) 1349.
18. *W.F. Piel et al.* Phys. Rev. C23 (1981) 708.
19. *S.T. Belaev.* Nucl. Phys. 64 (1965) 17.
20. *V.G. Zelevinsky.* Izvestia Acad. Nauk, ser. fiz. 48 (1984) N10.
21. *T. Tamura, K. Weeks and T. Kishimoto.* Nucl. Phys. A347 (1980) 359.
22. *R.F. Casten.* Nucl. Phys. A347 (1980) 173.
23. *M. Sakai.* Preprint INS-J-161. Tokyo, 1981.
24. *J.A. Grau et al.* Phys. Rev. C14 (1976) 2297.
25. *Yu.Yu. Zykov and G.I. Sychikov.* Preprint 11-83, Nuclear Physics Institute. Alma-Ata (1983).
26. *G.A. Shevelev et al.* Izvestia Acad. Nauk, ser. fiz. 42 (1978) 2617.
27. *B.E. Stepanov.* Yad. Fiz. 18 (1973) 99.

Table 1

J R_J	Harmonic limit	^{100}Pd (exp)	Eq. (11)	^{102}Pd (exp)	$\sigma_J = \frac{R_J - R_J^{00}}{J(J+1)}$
4	2	2.13	2.09	2.29	0.010
6	3	3.29	3.26	3.79	0.013
8	4	4.49	4.50	5.41	0.013
10	5	5.82	5.81	7.17	0.012
12	6	7.16	7.17	9.08	0.012
14	7	8.58	8.58	11.03	0.011

Table 2

J \ A	98	100	102	104	106	108	110
1	2	3	4	5	6	7	8
2^+_β			3.85 3.49 3.81		3.89 3.73^*_c 3.70	3.89 3.32 3.44	3.92 3.93^* 3.99
0^+_β			2.55 2.86 2.41	2.55 2.40 2.40	2.55 2.22 2.26	2.55 2.43 2.08	2.55 2.53 2.45
0^+_Δ			3.26 2.98_b 3.23	3.26 3,23 3.34	3.26 3.33 3.38	3.26 3.03 3.02	3.26 3.13 3.20
8^+_X							7.47 7.42 7.58
6^+_X							5.47 5.51 5.37
5^+_Z				4.95 4.99_b 5.03	5.04 5.39 5.13		
4^+_X			3.51 3.84 3.35		3.62 3.77 3.55		3.72 3.74 3.52
3^+_Z		3.26 3.55 3.22	3.41 3.80 3.28	3.44 3.28 3.41	3.47 3.04 3.45	3.30 3.08 3.19	3.54 3.24 3.34

1	2	3	4	5	6	7	8
2^+_X		2.09 2.39 2.07	2.17 2.76 2.06	2.18 2.41 2.09	2.20 2.20 2.10	2.20 2.15 1.95	2.23 2.18 2.00
14^+_Y		8.58 8.58 8.84	11.18 11.18^*_a 11.67				
12^+_Y		7.17 7.16 6.96	9.10 9.09 8.78		9.99 9.98^*_a 10.13		
10^+_Y		5.81 5.82 5.64	7.17 7.18 6.85	7.45 7.24 7.52	7.79 7.71^*_a 7.75		8.34 8.38 8.45
8^+_Y	4.16 4.21 4.14	4.50 4.49 4.38	5.39 5.42 5.11	5.57 5.80 5.51	5.80 5.79 5.65		6.16 6.14 6.07
6^+_Y	3.06 3.05 3.08	3.26 3.29 3.19	3.78 3.79 3.55	3.89 4.05 3.76	4.02 4.06 3.83	4.06 4.08 4.07	4.23 4.21 4.04
4^+_Y	2.00 1.86 2.04	2.09 2.13 2.06	2.33 2.29 2.19	2.39 2.38 2.25	2.45 2.40 2.28	2.47 2.42 2.36	2.55 2.46 2.35

Comments to tables

Table 2. Low-lying collective levels of Pd isotopes (in each triplet the middle value is experimental one [23], levels a, b and c corresponds to Refs [24], [25] and [26] respectively; the upper value is obtained from our formulae (9—12) and the lower one from the IBA-fit (13)). There are some cases (marked with asterisks) where we have chosen for comparison levels which agree with our systematics. For example, other candidates known in ^{106}Pd and ^{110}Pd have $R_{2\beta}=3.05$ and 3.25 correspondingly being probably of noncollective nature.

Table 3.

A	β_4^{exp}	β_2^{exp}	β_0^{exp}	β_4^{th}	β_2^{th}	β_0^{th}	$\varkappa$	$k\omega_0$
102	1.63 1.24(62)	0.43 1.13(62)		1.73	1.35	0.15	—0.25	0.005
104	1.46	0.81		1.80	1.45	0.35	—0.20	0.005
106	1.77 1.53(17) 1.60(30)	1.10 1.55	0.73 0.63	1.88	1.56	0.62	—0.14	0.005
108	1.92 1.84(18) 1.9(3)	1.70 1.8(4)	0.92 0.9(2) 0.87(17)	1.95	1.65	0.95	—0.07	0.005
110	1.80 1.68(17) 1.80(37)	1.05 1.25	0.67 0.57(15) 0.63(9)	1.87	1.54	0.58	—0.15	0.005

Table 3. Relative reduced transition probabilities $\beta_J = \frac{B(E2; J^+ \to 2_1^+)}{B(E2; 2_1^+ \to 0_1^+)}$ from two-phonon states $J=0$, 2, 4 for $^{102-110}$Pd isotopes: columns 2, 3 and 4—experimental data (upper value from Ref.[7] and lower one from Ref.[27]); columns 5, 6 and 7—calculated values according eqs (18—21); columns 8 and 9—adopted values of parameters $\varkappa$ and $k\omega_0$.

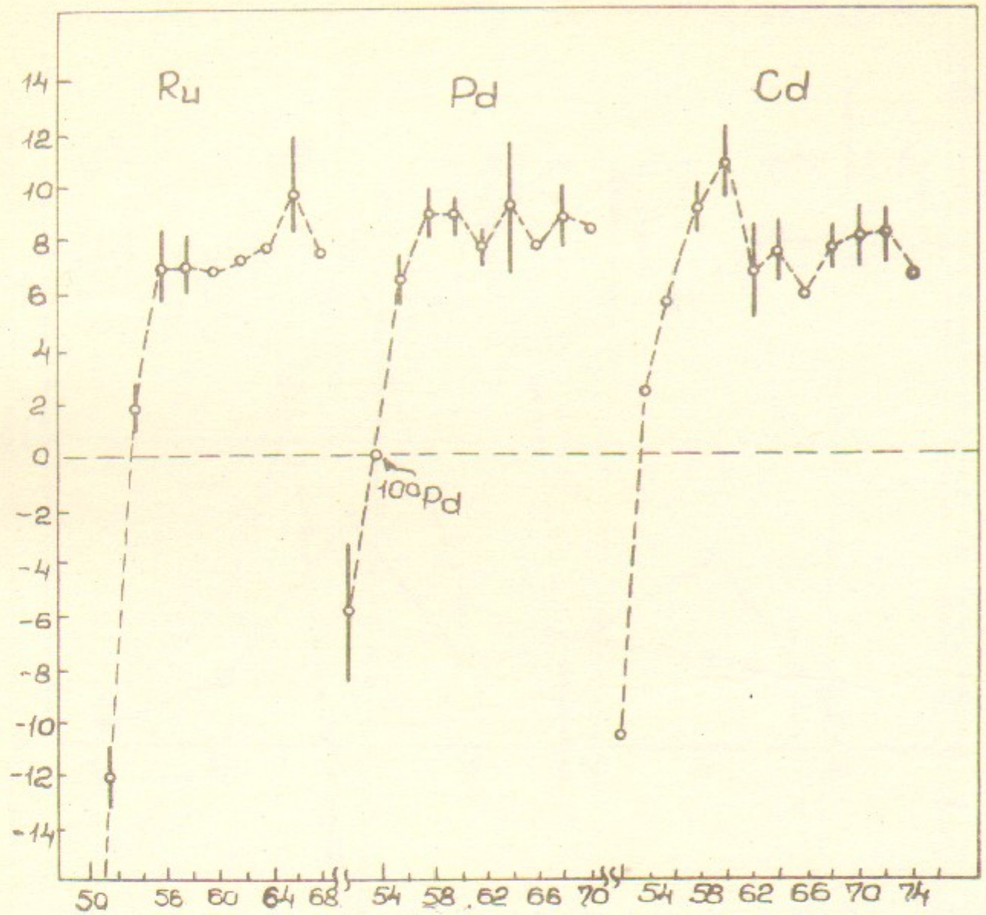

Fig.1. The energy parameter $w = \sigma(E_2 - E_0)$ keV for soft spherical nuclei Ru, Pd and Cd as a function of the neutron number.

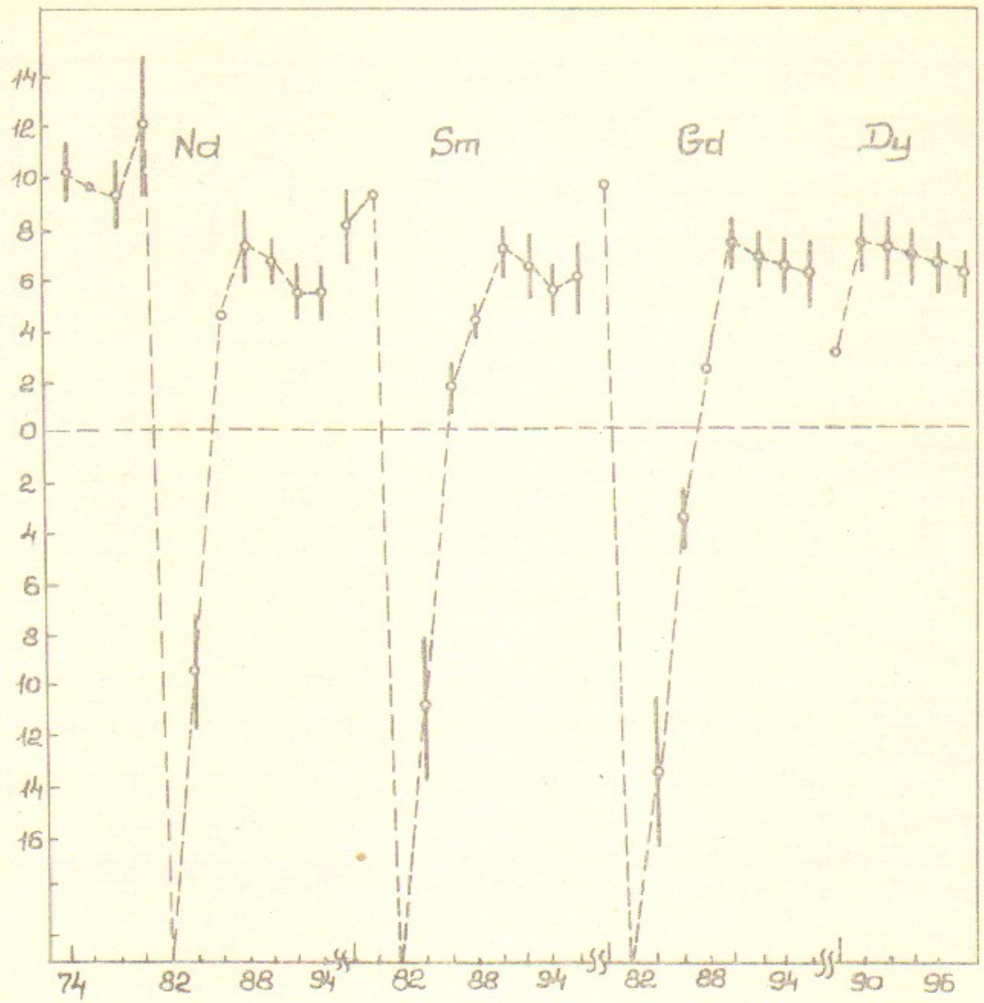

Fig.2. The energy parameter $\omega = \sigma(E_2 - E_0)$ keV for transitional and deformed nuclei Ne, Sm, Gd and Dy as a function of neutron number.

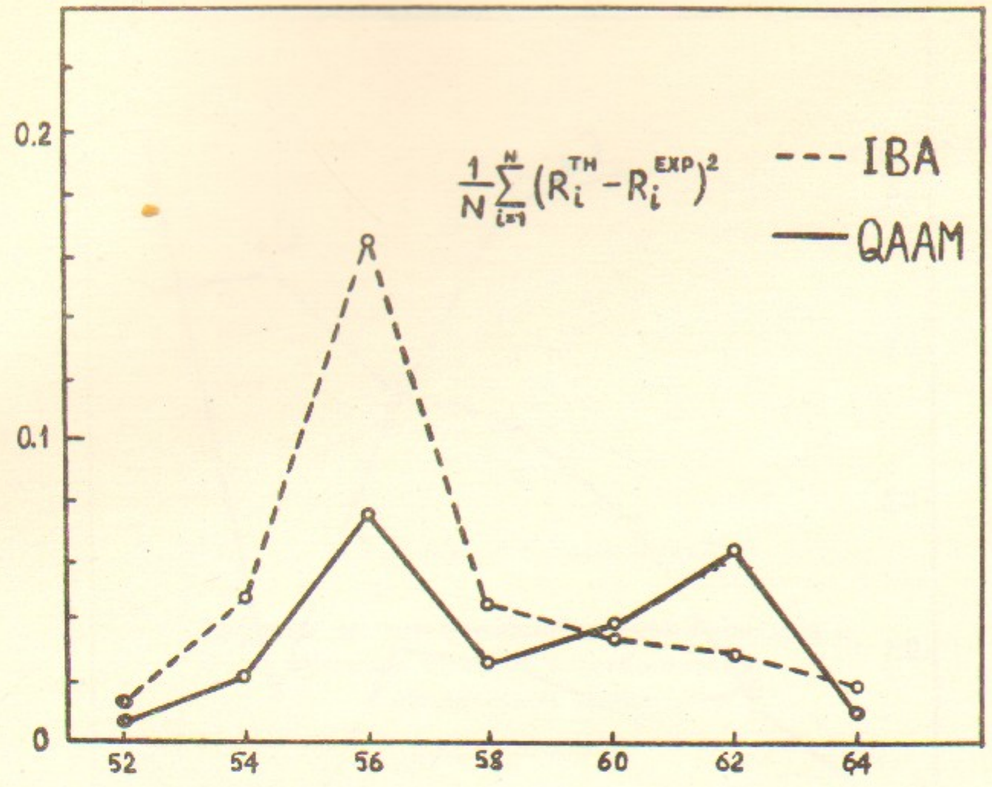

Fig.3. The mean square deviation of energy ratios of $^{98-110}$Pd isotopes $\frac{1}{N}\sum_{i=1}^{N}(R_i^{th}-R_i^{exp})^2$ as a function of the neutron number for QAAM calculations (solid line) and for the IBA-fit (dashed line).

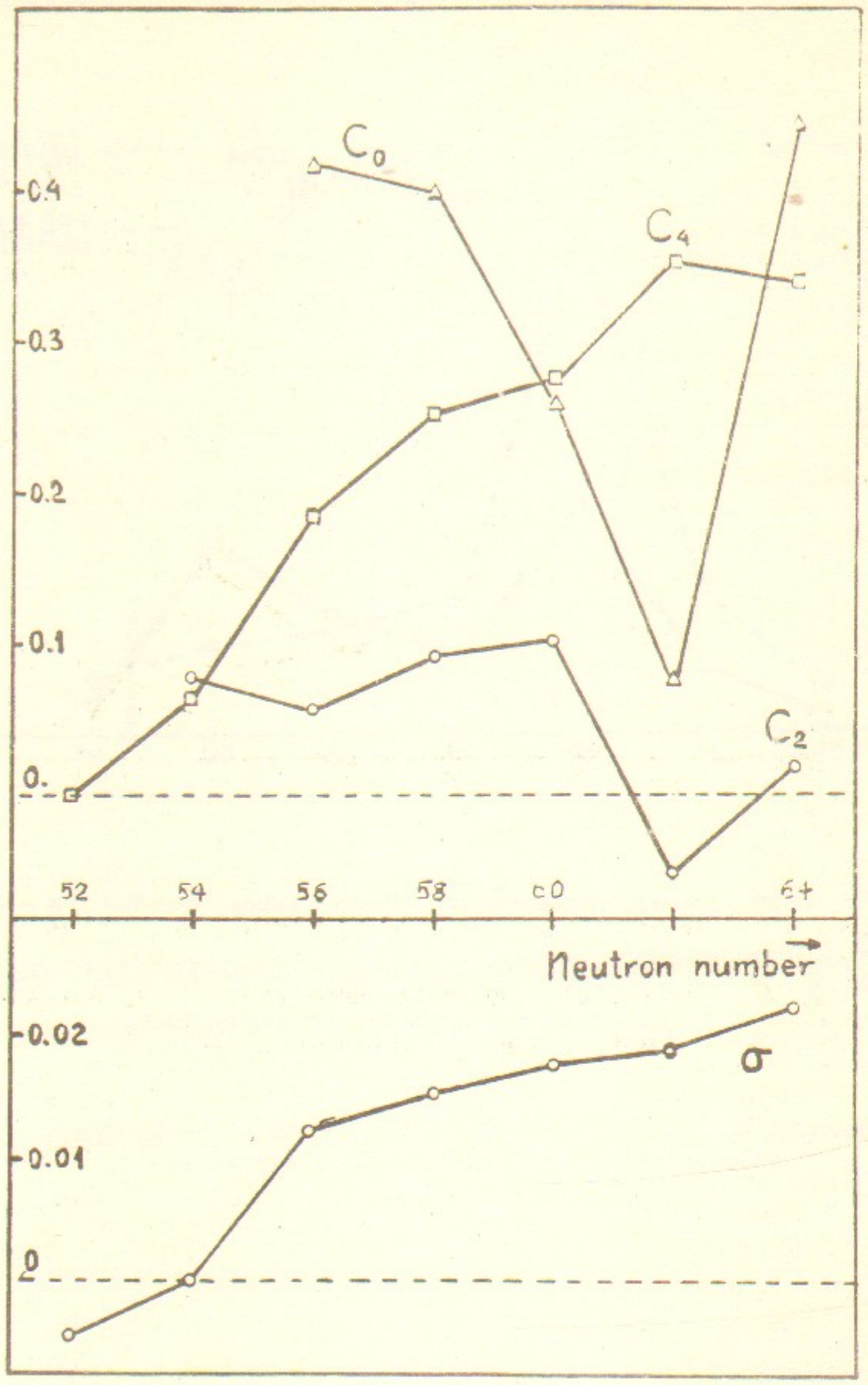

Fig.4. Values of the parameter σ in the QAAM model (lower part) and of the parameters C_0, C_2 and C_4 for IBA (upper part) as functions of the neutron number for $_{46}$Pd isotopes.

О.К.Воров, В.Г.Зелевинский

Эффекты четырехфононной ангармоничности и углового момента в четно-четных сферических ядрах

Препринт 84-137

Ответственный за выпуск С.Г.Попов

Подписано в печать 19 сентября 1984 г. МН 04551
Формат бумаги 60×90 1/16 Объем 1,7 печ.л., 1,4 уч.-изд.л.
Тираж 290 экз. Бесплатно. Заказ № 137

Набрано в автоматизированной системе на базе фотонаборного автомата ФА1000 и ЭВМ «Электроника» и отпечатано на ротапринте Института ядерной физики СО АН СССР,
Новосибирск, 630090, пр. академика Лаврентьева, 11.